



Cite this: *Chem. Commun.*, 2023, 59, 7827

Received 11th April 2023,
Accepted 22nd May 2023

DOI: 10.1039/d3cc01472j

rsc.li/chemcomm

A general scheme for generating NMR supersequences combining high- and low-sensitivity experiments†

Jonathan R. J. Yong,^a Ēriks Kupče^b and Tim D. W. Claridge^{ib}*^a

NOAH supersequences are a way of collecting multiple 2D NMR experiments in a single measurement. So far, this approach has been limited to experiments with comparable sensitivity. Here, we propose a scheme which overcomes this limitation, combining experiments with very different sensitivities such as 1,1-ADEQUATE, ¹⁵N HMBC, and ¹³C HSQC.

Nuclear magnetic resonance (NMR) spectroscopy plays a key role in the structural elucidation of natural products; in particular, two-dimensional (2D) NMR experiments provide vast amounts of information on through-bond and through-space molecular connectivity.^{1,2} However, these experiments are often time-consuming as they require the incrementation of indirect-dimension evolution periods in order to construct the requisite 2D data matrices. One particularly flexible method for accelerating 2D data acquisition is the NOAH (NMR by Ordered Acquisition using ¹H detection) technique,^{3,4} in which multiple 2D experiments ('modules') are combined into a single experiment using only a single recovery delay. These nested 'supersequences', which rely on the tailored excitation of magnetisation from different isotopologues, provide an array of 2D spectra (up to 10 so far⁵) in greatly reduced experiment times.

Virtually all common 2D experiments, such as HSQC, HMQC, COSY, TOCSY, and NOESY, have been exploited in NOAH supersequences, allowing for the (manual or computer-assisted) structural elucidation of a wide range of molecules.^{5–8} However, such experiments tend to fall short in proton-sparse molecules^{9–11} as they do not yield sufficient correlations. In such cases, additional information may be obtained through the HMBC^{12–14} and HSQMBC^{15,16} experiments which detect long-range X–¹H couplings (ⁿJ_{XH}, X = ¹³C or ¹⁵N). Although these tend to yield vastly more correlations, there may remain ambiguity in

interpreting the resulting data as these techniques do not reveal the exact number of bonds over which a coupling is mediated. In contrast, one-bond ¹³C–¹³C correlations (¹J_{CC}), obtained through the INADEQUATE¹⁷—or more practically, ADEQUATE^{18,19}—experiments, allow chemists to directly trace out carbon backbones with much greater certainty. The main limitation of such experiments is their low sensitivity, as they rely on pairs of heteronuclei with low natural abundances; nonetheless, with the introduction of cryogenically cooled probes and concomitant advances in achievable signal-to-noise ratios (SNRs), such experiments can nowadays be feasibly run even on relatively dilute samples.

To date, insensitive experiments such as ¹⁵N HMBC and ADEQUATE have not been the main focus of NOAH supersequences.²⁰ This is because in a traditional 'linear' supersequence, each constituent module is recorded with the same number of transients. For dilute samples, the total experiment duration is therefore dictated by the module with the lowest sensitivity, and higher-sensitivity modules (e.g. HSQC or COSY) would be recorded with more transients than strictly necessary. Although the more sensitive modules would still be obtained 'for free', the *effective* time savings thus realised are smaller than for a supersequence constructed from modules with balanced sensitivities.

For this reason, the low-sensitivity ADEQUATE and ¹⁵N HMBC modules (respectively abbreviated as 'A' and 'B_N') form a natural pairing in the NOAH-2 AB_N supersequence introduced here (Fig. 1b). However, in this work, we also go beyond the traditional 'linear' or 'horizontal' model of a supersequence in adding more modules through 'vertical' interleaving, in a similar fashion to the parallel supersequences recently described.⁵ We show that, following an initial ADEQUATE module, up to four modules (¹⁵N HMBC, ¹³C HMBC, ¹⁵N sensitivity-enhanced HSQC (seHSQC), and ¹³C HSQC) may be interleaved in this 'vertical' fashion (Fig. 1d and e), yielding five modules with balanced intensities and high-quality data. By tailoring the number of times each module is acquired, this technique provides a powerful and flexible way to balance

^a Chemistry Research Laboratory, Department of Chemistry, University of Oxford, Mansfield Road, Oxford, OX1 3TA, UK. E-mail: tim.claridge@chem.ox.ac.uk

^b Bruker UK Ltd, R&D, Coventry CV4 9GH, UK

† Electronic supplementary information (ESI) available. See DOI: <https://doi.org/10.1039/d3cc01472j>



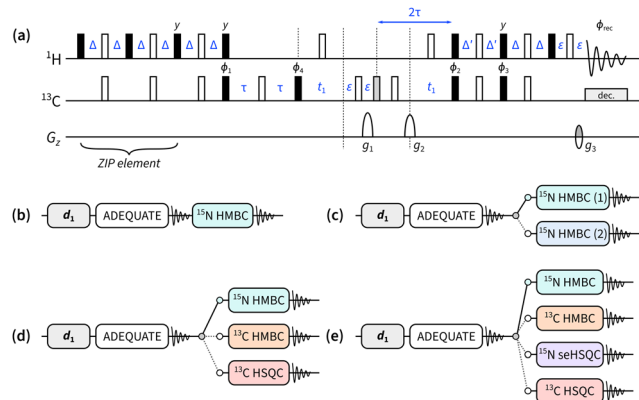


Fig. 1 Pulse sequences described in this work. (a) ZIP-1,1-ADEQUATE module. Filled and empty bars refer to 90° and 180° pulses respectively; the grey filled bar is a 120° pulse for ^{13}C double-quantum to single-quantum coherence transfer.²¹ Pulse and receiver phases are: $\phi_1 = x, -x$; $\phi_2 = 2(x), 2(-x)$; $\phi_3 = 2(y), 2(-y)$; $\phi_4 = 4(x), 4(-x)$; $\phi_{\text{rec}} = x, -x, -x, x, -x, x, x, -x$. Delays are set as follows: $\Delta = 1/(4 \cdot J_{\text{CH}})$, $\Delta' = 1/(8 \cdot J_{\text{CH}})$, and $\tau = 1/(4 \cdot J_{\text{CC}})$. ε is the minimum time required for a pulsed field gradient and the following recovery delay. Gradient amplitudes as a percentage of the maximum amplitude are: $g_1 = 78.5\%$, $g_2 = 77.6\%$, and $g_3 = -59\%$. Echo-antiecho selection is achieved by inverting the sign of g_3 as well as the pulse phase ϕ_3 . (b) NOAH-2 AB_N supersequence. (c) p -NOAH-3 $\text{A}(\text{B}_\text{N}/\text{B}_\text{N})$, where the two ^{15}N HMBC experiments are optimised for two different values of $^nJ_{\text{NH}}$. (d) p -NOAH-4 $\text{A}(\text{B}_\text{N}/\text{B}/\text{S})$. (e) p -NOAH-5 $\text{A}(\text{B}_\text{N}/\text{B}/\text{S}_\text{N}^+/\text{S})$.

modules with different sensitivities, and fully generalises our previous work on parallel supersequences, which only ‘vertically’ interleaved two modules at a time.

When designing NMR supersequences, it is generally a good rule of thumb to place the module with the lowest sensitivity first: this is because any incomplete preservation of magnetisation by earlier modules will lead to decreased sensitivity in later modules. The 1,1-ADEQUATE module, which relies on neighbouring pairs of ^{13}C nuclei—occurring only in roughly 1 out of 8130 molecules—is therefore placed at the beginning of all the supersequences described here.

The ADEQUATE module (Fig. 1a) is designed to only use the magnetisation of protons directly bonded to ^{13}C , which we denote here as $^1\text{H}^{\text{IC}}$.^{22,23} In order to maintain the sensitivity of later modules, it must return the magnetisation of all other protons (denoted as $^1\text{H}^{\text{IC}}$; *i.e.* those not bonded to ^{13}C) to the equilibrium $+z$ state. This is accomplished by replacing the initial 90° excitation pulse by the zz isotope-selective pulse element (ZIP),^{23,24} which effects 90°_{-x} and 90°_{-y} rotations on $^1\text{H}^{\text{IC}}$ and $^1\text{H}^{\text{IC}}$ magnetisation respectively. (Other isotope-specific elements such as BANGO^{25–27} may also be used here, with similar results generally being obtained.²³) The ^{15}N HMBC module of choice is a simple magnitude-mode version, with an optional first-order low-pass J -filter. In the NOAH-2 AB_N supersequence (Fig. 1b), this module simply consumes the remaining $^1\text{H}^{\text{IC}}$ magnetisation which was preserved by the ZIP-ADEQUATE module.

Although this NOAH-2 AB_N sequence performs well on its own (Fig. 2), it suffers from the drawback that the ^{15}N HMBC is optimised for one specific value of $^nJ_{\text{NH}}$. In practice, $^nJ_{\text{NH}}$ values range from 2–16 Hz; in a single HMBC experiment, some correlations may therefore be lost due to J -coupling mismatch.

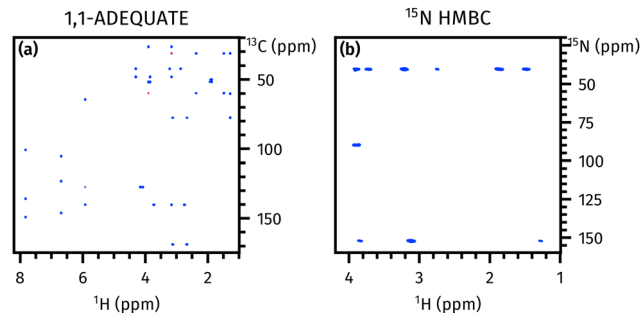


Fig. 2 Spectra obtained from the NOAH-2 AB_N supersequence. (a) 1,1-ADEQUATE. (b) ^{15}N HMBC. Spectra were obtained on a 700 MHz Bruker AV III equipped with a TCI H/C/N cryoprobe; the sample used was 50 mM brucine in CDCl_3 (see Fig. S2 for structure, ESI†).

To circumvent this issue, a variety of accordion-type experiments^{28–30} have been designed which decrement the J -evolution period in step with t_1 , allowing a wider range of couplings to be sampled. Alternatively, and perhaps more commonly, two (or more) separate HMBC experiments, optimised for different $^nJ_{\text{NH}}$ values, can be recorded; the resulting spectra may be co-added to mimic an accordion-type HMBC if desired. These separate HMBC modules cannot be recorded sequentially, as they both draw on the same $^1\text{H}^{\text{IC}}$ magnetisation. However, they can easily be executed in an interleaved or parallel manner where, after the ADEQUATE module, the two HMBC experiments are alternately acquired.⁵ In Fig. 1c, this is illustrated by a ‘vertical’ stacking of the two modules to form a parallel (p)-NOAH-3 $\text{A}(\text{B}_\text{N}/\text{B}_\text{N})$ supersequence. Thus, after each odd-numbered increment of the ADEQUATE, the first HMBC is acquired; and after each even-numbered increment, the second HMBC is acquired. This means that both HMBC spectra have half the usual number of t_1 increments compared to the ADEQUATE, which is acceptable since the ^{15}N dimension is typically sparse and a high resolution is not required; furthermore, since the ^{15}N HMBC is more sensitive than the ADEQUATE, the reduced number of FIDs recorded per HMBC is practically inconsequential. As can be seen in Fig. 3, the two HMBC spectra reveal different sets of correlations, allowing for more confident structural determination.

In the above $\text{A}(\text{B}_\text{N}/\text{B}_\text{N})$ experiment and in previous work,⁵ we have shown how two alternating modules can be used to construct parallel supersequences. This concept can naturally be further generalised in order to allow two or more different experiments to be acquired alternately as the second module in the supersequence. These interleaved experiments can be arranged such that they each have lower resolution compared to the first module (as was done here), or such that they each have a fewer number of transients. In principle, such an arrangement can be used for all modules in a supersequence, not just the second module as is done here. However, it is important to remember that earlier modules affect the amount of magnetisation passed on to the later modules; thus, interleaving later modules in a sequence usually leads to more robust supersequences with minimal discrepancies in data intensity or spectral quality.



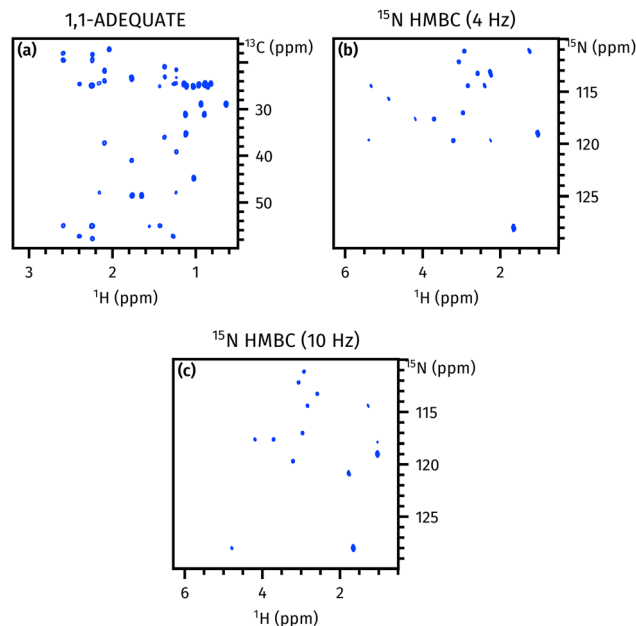


Fig. 3 Spectra obtained from the *p*-NOAH-3 A(B_N/B_N) supersequence. (a) 1,1-ADEQUATE (256 *t*₁ increments). (b) ¹⁵N HMBC optimised for $^nJ_{\text{NH}} = 4$ Hz (128 *t*₁ increments). (c) ¹⁵N HMBC optimised for $^nJ_{\text{NH}} = 10$ Hz (128 *t*₁ increments). Spectra were obtained on a 700 MHz Bruker AV III equipped with a TCI H/C/N cryoprobe; the sample used was 50 mM cyclosporin A in C₆D₆ (see Fig. S5 for structure, ESI†).

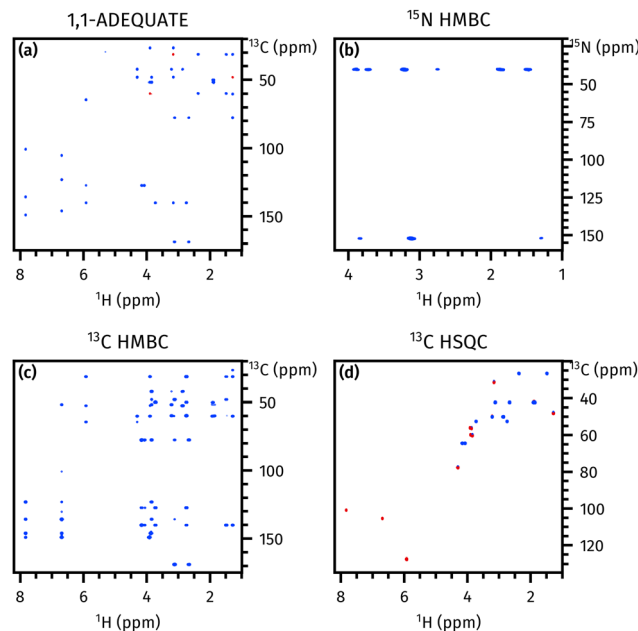


Fig. 4 Spectra obtained from the *p*-NOAH-4 A(B_N/B/S) supersequence. All modules were recorded with 256 *t*₁ increments. (a) 1,1-ADEQUATE (16 transients). (b) ¹⁵N HMBC (12 transients). (c) ¹³C HMBC (2 transients). (d) ¹³C HSQC (2 transients). Spectra were obtained on a 700 MHz Bruker AV III equipped with a TCI H/C/N cryoprobe; the sample used was 50 mM brucine in CDCl₃.

In the *p*-NOAH-4 A(B_N/B/S) supersequence (Fig. 1d), the ADEQUATE module is followed by one of three choices: a ¹⁵N HMBC, a ¹³C HMBC (denoted B), or a ¹³C HSQC (denoted S). Because these three latter modules do not have the same intrinsic sensitivity, we balance this by allocating a different number of transients to each module. In this specific example, each *t*₁ increment of the ADEQUATE collects a total of 8*n* transients (where *n* is some positive integer); the ¹⁵N HMBC 6*n* transients; and the ¹³C HMBC and HSQC *n* transients each. The value of *n* is chosen to ensure that all spectra have sufficient sensitivity; the spectra in Fig. 4 were acquired with *n* = 2. The exact number of transients for each module can be customised *via* user-defined constants in the provided pulse programmes. The exact implementation of these supersequences is described in detail in Section S1, and instructions for obtaining the pulse programmes in Section S2 (ESI†).

The acquisition of the *p*-NOAH-4 A(B_N/B/S) spectra in Fig. 4 took 124 minutes; in contrast, normal acquisition of all four experiments (with the equivalent number of transients per module) required a total of 223 minutes. As the ADEQUATE is placed first in the supersequence, its sensitivity is almost identical to that of a standalone ADEQUATE; the inclusion of the ZIP element causes only an approximate 5% loss. The ¹⁵N and ¹³C HMBC spectra experience small losses (16–29%) in sensitivity, due to imperfect magnetisation retention by the ADEQUATE module. This is, however, outweighed by the almost twofold time savings provided by concatenation of the modules: if the NOAH supersequence were acquired for as long as the standalone experiments were, the ¹⁵N HMBC spectra would have almost

the same SNR, and the ¹³C HMBC from the NOAH would in fact have a 12% improvement in SNR. Due to the reuse of ¹H^C magnetisation, the HSQC module only retains 29% of its original sensitivity. However, as the HSQC is still two orders of magnitude more sensitive than the ADEQUATE, this decrease is readily tolerated; if necessary, the sensitivity-enhanced HSQC module^{23,24} may also be used in its place.

While this combination of modules proves to be particularly elegant in that it furnishes virtually all heteronuclear correlations needed for structural assignment of nitrogen-containing organic molecules, it is by no means the only valid one. The principle of interleaved modules can be used to incorporate almost any experiment that may be required: as an example, spectra from a *p*-NOAH-4 A(B_N/N/S) experiment (N = NOESY, replacing the ¹³C HMBC) are shown in Fig. S3 (ESI†).

As a final example, we add a further ¹⁵N seHSQC (S⁺_N) module to the above sequence. The ¹⁵N seHSQC uses only ¹H^N magnetisation (*i.e.* protons directly bonded to ¹⁵N), which is separate from all other magnetisation pools introduced so far. Thus, in principle, it can simply be added *linearly* as a third sequential module to the supersequence: such an arrangement would maximise its sensitivity as the ¹⁵N seHSQC data are collected on every scan in the supersequence. Such an arrangement would, however, compromise the performance of the other modules, as they must then be modified to preserve the requisite ¹H^N magnetisation: for example, the HMBC modules would need to be modified to include the *zz*-filter,^{6,7} which leads to further sensitivity losses. Instead of this, the ¹⁵N seHSQC can most efficiently be implemented in a ‘vertical’, interleaved manner, by simply reducing



the number of transients for the ^{15}N HMBC by n and diverting these towards the ^{15}N seHSQC. This means that the second slot in the supersequence now alternates between four different experiments, as shown in Fig. 1e. This example especially illustrates how the use of interleaved and sequential acquisition leads to much greater flexibility in supersequence design, especially when considering the relative sensitivities of different modules.

The five spectra obtained from this sequence are shown in Fig. S6 (ESI†). Collectively, this supersequence provides virtually all heteronuclear correlation data required for structural elucidation or assignment. These can further be processed using covariance techniques^{31–33} to yield double-heteronuclear correlation spectra (Section S6, ESI†). This supersequence is similar in spirit to the PANACEA experiment,^{34,35} but yields greater sensitivity as it uses equilibrium ^1H magnetisation rather than the low-magnetogyric ratio ^{13}C and ^{15}N nuclei, and does not require multiple-receiver hardware.^{4,36} Of course, the ADEQUATE experiment may not be necessary for every novel compound encountered. However, in cases where it is needed, the supersequences described here demonstrate that other valuable heteronuclear spectra can also be acquired together with the ADEQUATE in a manner which yields significant time savings and sensitivity per unit time improvements.

In conclusion, we have demonstrated here how low-sensitivity experiments, such as 1,1-ADEQUATE and ^{15}N HMBC, may be optimally combined in NMR supersequences, leading to substantial reductions in experiment time. Through a generalisation of our previous concept of parallel supersequences, further high-sensitivity modules may be added to the supersequence both ‘horizontally’ and ‘vertically’, corresponding respectively to sequential and interleaved/parallel acquisition. The spectra thus obtained provide the chemist with far more powerful tools for the characterisation of complex molecules, especially in cases where existing (sequential) NOAH supersequences do not provide sufficient information for unambiguous assignment. A notable example of this is proton-sparse nitrogen heterocycles, which are commonly found in pharmaceuticals. The pulse programmes and processing scripts used in this work can be obtained *via* the Bruker User Library or GitHub; links are provided in Section S2 of the ESI.†

We thank Dr Mohammadali Foroozandeh (University of Oxford) for helpful discussions. J. R. J. Y. thanks the Clarendon Fund (University of Oxford) and the EPSRC Centre for Doctoral Training in Synthesis for Biology and Medicine (EP/L015838/1) for a studentship, generously supported by AstraZeneca, Diamond Light Source, Defence Science and Technology Laboratory, Evotec, GlaxoSmithKline, Janssen, Novartis, Pfizer, Syngenta, Takeda, UCB, and Vertex.

Conflicts of interest

There are no conflicts of interest to declare.

Notes and references

- 1 M. Findeisen and S. Berger, *50 and More Essential NMR Experiments: A Detailed Guide*, Wiley, Weinheim, 2013.
- 2 T. D. W. Claridge, *High-Resolution NMR Techniques in Organic Chemistry*, Elsevier, Amsterdam, 3rd edn, 2016.
- 3 Ě. Kupĉe and T. D. W. Claridge, *Angew. Chem., Int. Ed.*, 2017, **56**, 11779.
- 4 Ě. Kupĉe, L. Frydman, A. G. Webb, J. R. J. Yong and T. D. W. Claridge, *Nat. Rev. Methods Primers*, 2021, **1**, 27.
- 5 Ě. Kupĉe, J. R. J. Yong, G. Widmalm and T. D. W. Claridge, *JACS Au*, 2021, **1**, 1892.
- 6 Ě. Kupĉe and T. D. W. Claridge, *Chem. Commun.*, 2018, **54**, 7139.
- 7 Ě. Kupĉe and T. D. W. Claridge, *J. Magn. Reson.*, 2019, **307**, 106568.
- 8 J. R. J. Yong, Ě. Kupĉe and T. D. W. Claridge, *Anal. Chem.*, 2022, **94**, 2271.
- 9 K. N. White, T. Amagata, A. G. Oliver, K. Tenney, P. J. Wenzel and P. Crews, *J. Org. Chem.*, 2008, **73**, 8719.
- 10 M. M. Senior, R. T. Williamson and G. E. Martin, *J. Nat. Prod.*, 2013, **76**, 2088.
- 11 A. V. Buevich, R. T. Williamson and G. E. Martin, *J. Nat. Prod.*, 2014, **77**, 1942.
- 12 A. Bax and M. F. Summers, *J. Am. Chem. Soc.*, 1986, **108**, 2093.
- 13 R. C. Crouch, W. Llanos, K. G. Mehr, C. E. Hadden, D. J. Russell and G. E. Martin, *Magn. Reson. Chem.*, 2001, **39**, 555.
- 14 G. E. Martin and A. J. Williams, *Annu. Rep. NMR Spectrosc.*, 2015, **84**, 1.
- 15 R. T. Williamson, A. V. Buevich, G. E. Martin and T. Parella, *J. Org. Chem.*, 2014, **79**, 3887.
- 16 L. Castaňar, J. Sauri, R. T. Williamson, A. Virgili and T. Parella, *Angew. Chem., Int. Ed.*, 2014, **53**, 8379.
- 17 A. Bax, R. Freeman and T. A. Frenkiel, *J. Am. Chem. Soc.*, 1981, **103**, 2102.
- 18 B. Reif, M. Köck, R. Kerssebaum, H. Kang, W. Fenical and C. Griesinger, *J. Magn. Reson., Ser. A*, 1996, **118**, 282.
- 19 G. E. Martin, *Annu. Rep. NMR Spectrosc.*, 2011, **74**, 215.
- 20 V. M. Rao Kakita and R. V. Hosur, *RSC Adv.*, 2020, **10**, 21174.
- 21 T. H. Mareci and R. Freeman, *J. Magn. Reson.*, 1982, **48**, 158.
- 22 J. Orts and A. D. Gossert, *Methods*, 2018, **138–139**, 3.
- 23 J. R. J. Yong, A. L. Hansen, Ě. Kupĉe and T. D. W. Claridge, *J. Magn. Reson.*, 2021, **329**, 107027.
- 24 A. L. Hansen, Ě. Kupĉe, D.-W. Li, L. Bruschweiler-Li, C. Wang and R. Bruschweiler, *Anal. Chem.*, 2021, **93**, 6112.
- 25 O. W. Sørensen, *Bull. Magn. Reson.*, 1994, **16**, 49.
- 26 T. M. Nagy, T. Gyöngyösi, K. E. Kövér and O. W. Sørensen, *Chem. Commun.*, 2019, **55**, 12208.
- 27 T. M. Nagy, K. E. Kövér and O. W. Sørensen, *Angew. Chem., Int. Ed.*, 2021, **60**, 13587.
- 28 R. Wagner and S. Berger, *Magn. Reson. Chem.*, 1998, **36**, S44.
- 29 C. E. Hadden, G. E. Martin and V. V. Krishnamurthy, *J. Magn. Reson.*, 1999, **140**, 274.
- 30 C. E. Hadden, G. E. Martin and V. V. Krishnamurthy, *Magn. Reson. Chem.*, 2000, **38**, 143.
- 31 F. Zhang and R. Bruschweiler, *J. Am. Chem. Soc.*, 2004, **126**, 13180.
- 32 D. A. Snyder and R. Bruschweiler, *J. Phys. Chem. A*, 2009, **113**, 12898.
- 33 M. Jaeger and R. L. E. G. Aspers, *Annu. Rep. NMR Spectrosc.*, 2014, **83**, 271.
- 34 Ě. Kupĉe and R. Freeman, *J. Am. Chem. Soc.*, 2008, **130**, 10788.
- 35 Ě. Kupĉe and R. Freeman, *J. Magn. Reson.*, 2010, **206**, 147.
- 36 Ě. Kupĉe, K. R. Mote, A. Webb, P. K. Madhu and T. D. W. Claridge, *Prog. Nucl. Magn. Reson. Spectrosc.*, 2021, **124–125**, 1.

